

## Tidally-modulated high frequency internal waves in Gautami-Godavari estuary, East coast of India

B.Sridevi<sup>1</sup>, \*T.V.Ramana Murty<sup>1</sup>, Y.Sadhuram<sup>1</sup>, V.V.S.S.Sarma<sup>1</sup>, V.S.N.Murty<sup>1</sup> & K.V.S.R.Prasad<sup>2</sup>

<sup>1</sup>National Institute of Oceanography (CSIR), Regional Centre, 176, Lawsons Bay Colony, Visakhapatnam, India

<sup>2</sup>Dept. Meteorology & Oceanography, Andhra University, Visakhapatnam, India

\*[E-Mail : [tvrmurty@nio.org](mailto:tvrmurty@nio.org)]

Received 26 June 2013 ; revised 7 July 2013

Time series temperature and salinity (at 1 hour interval) and currents data (10 min interval) at surface (3 m) and bottom (14 m), collected in the Gautami-Godavari estuary during 25-27 September 2008 were utilized to document the characteristics of Internal waves (IW) and to infer their generation mechanism. Based on the stability criteria, two High Frequency (HF) significant modes in the Internal Wave (IW) field at frequencies 96.67 cph (10 m depth) and 71.15 cph (14 m depth) have been identified. At these modes, IW parameters viz., wave length ( $L$ ), wave number ( $\kappa$ ), potential energy ( $PE$ ), baroclinic potential energy ( $BPE$ ) and phase speed ( $c_i$ ) and displacement function ( $\eta(z,t)$ ) have been computed (with salinity and currents data) objectively by adopting well known harmonic technique through Principal Component Analysis (PCA). Results revealed that (1) first mode: IW was found to move with a phase speed of  $0.13 \text{ m s}^{-1}$  and wave length of  $0.0056 \text{ km}$  (wave number= $178.64 \text{ cycles km}^{-1}$ ) having energies of  $0.0006 \text{ J m}^{-2}$  (potential) and  $0.0027 \text{ J m}^{-2}$  (baroclinic) whereas (2) second mode:  $0.09 \text{ m s}^{-1}$ ,  $0.0076 \text{ km}$ ,  $131.48 \text{ cycles km}^{-1}$ ,  $0.0055 \text{ J m}^{-2}$ ,  $0.020 \text{ J m}^{-2}$  and  $0.094 \text{ m s}^{-1}$  for  $L$ ,  $\kappa$ ,  $PE$ ,  $BPE$  and  $c_i$  respectively.  $\eta(z,t)$  was found to be positive (elevation-type IWs) and negative values (oscillation-type) during IW propagation of two modes respectively wherein mode 2 is more energetic (8 times) than mode 1. Tidally-modulated force may be the possible mechanism to generate HF IWs under ebb period.

[Keywords: Godavari estuary, Stratification, High frequency internal waves]

### Introduction

Physical Oceanographers recognize that IW field as the main agent, or may be the only one, for mixing the interior of the ocean through the pycnocline<sup>1</sup>. In calm sea, the sea surface is marked by alternate smooth and rough bands – a phenomenon called slicks. The slicks are usually associated with the IW down below. Radar from the ship or Synthetic Aperture Radar (SAR) from a satellite can map the slicks by measuring the reflected or back scattered energy from these bands. The IWs are usually observed with SAR near coastal areas occurring in separate groups of 10 – 60 km apart with crests 10 – 100 km long. With increasing rate of coverage and higher sampling rate satellite may prove useful for studying coastal IW field, especially at tidal frequencies<sup>2</sup>. The IW frequencies are bounded by inertial frequency ( $f$ ) as the lower limit and Brunt-Vaisala frequency ( $N$ ) as the upper limit. The  $f$  is defined as  $f = 2\Omega \sin(\Phi)$ , where  $\Omega$  is the angular velocity of the earth's rotation and  $\Phi$  is the latitude. The IW spectrum in

the deep ocean has consistently the same shape wherever it is observed, except when the observations are made closer to a strong source of IWs<sup>3</sup>. Based on the field observations, Garrett and Munk<sup>4</sup> developed an energy-frequency spectrum, known as the Garrett-Munk (GM) spectrum of IWs. IWs evolve a wide spectrum of frequency scales, depending on their wavelength. In IW spectrum, the buoyancy frequency is the upper limit of wave frequencies,  $\omega$  that can propagate through a system. GM succeeded in modeling deep water IW and later it was modified for shallow water IW<sup>5</sup>. The IWs are broadly classified into low - frequency (LF) (<0.5 cph) and high – frequency (HF) (> 0.5 cph) waves<sup>6</sup>.

An insight into IWs in the seas around India has been broadly described by Murthy<sup>6</sup>. In the recent past some studies were done on IWs in the coastal waters of Bay of Bengal, utilizing the time series measurements from stationary ships and from the

oceanographic buoys<sup>7-13</sup>. Most of these studies revealed the IW parameters like amplitude, frequency, speed and direction, wavelength etc., and their variability with space and time in the coastal waters. The time series measurements made from stationary ships and from buoys at different places in the seas around India indicated prominent IW of tidal (0.05 cph) and high (0.5 - 10 cph) frequencies. The High Frequency (HF) IWs were found to exhibit diurnal variability with stronger activity during night time compared to day time under the influence of local winds. Recently, Sridevi et al.,<sup>12, 13</sup> deduced IW characteristics of coastal waters of Bay of Bengal from observed CTD and thermistor chain data on continental shelf and revealed that observed IW features in thermocline are well comparable with GM generated IW field than at the bottom. This could be due to the limitation of the model which considers linearity and hydrostatic approximation. HF IW observed at the bottom could be due to the advection of tidal current over the shallow irregular bottom in the presence of stratification. Generation of HF IW can be studied in the frame work of fully non-hydrostatic model. Rao et al.,<sup>14</sup> suggested that, even though there is wide variety of physical processes in oceans and many of them are adequately modeled with hydrostatic approximation, but HF IW contributes to the physics that influence mixing in a density stratified system and have been shown to be non-hydrostatic. Studies on IWs in partially mixed and stratified estuaries<sup>15, 16</sup>, Ems estuary (Germany)<sup>17</sup>, St. Lawrence estuary<sup>18</sup> and in fjords<sup>19</sup> have been reported earlier. To our knowledge, no attempt has been made so far to study this aspect in the Godavari estuary. Apart from low frequency (LF) IWs, exited HF IWs which are generated in riverine system as these transport fresh water plumes carrying disperse chemicals, dissolved substances, particulate matter, nutrients, heat and small organisms into the coastal waters and it is an important aspect for coastal zone management. HF IWs are more energetic in river plume than in the coastal ocean and these displace near-surface water particles into the deeper depths and generate strong currents and turbulence that mix nutrients into near surface waters for biological utilization. Such HF IW characteristics as source of high river discharge conditions have been studied elsewhere<sup>20, 21</sup>.

In the present study, time series CTD data (hourly) and currents (surface & bottom) (10 min)

collected during 25-27 September 2008 in Godavari estuary (Fig. 1) have been utilized to identify the generation and characteristics of HF IWs. Based on the spectrum, harmonic and stability subject to limited time series data, we have deduced IW characteristics and their mechanisms to generate under the influence of tidal forces with salt wedge and heavy fresh water discharge conditions. Principal Component Analysis (PCA) method has been applied which can be an alternative method while performing harmonic analysis to deduce HF IW characteristics. The complete methodology and relevant mathematics have been presented below for the present context.

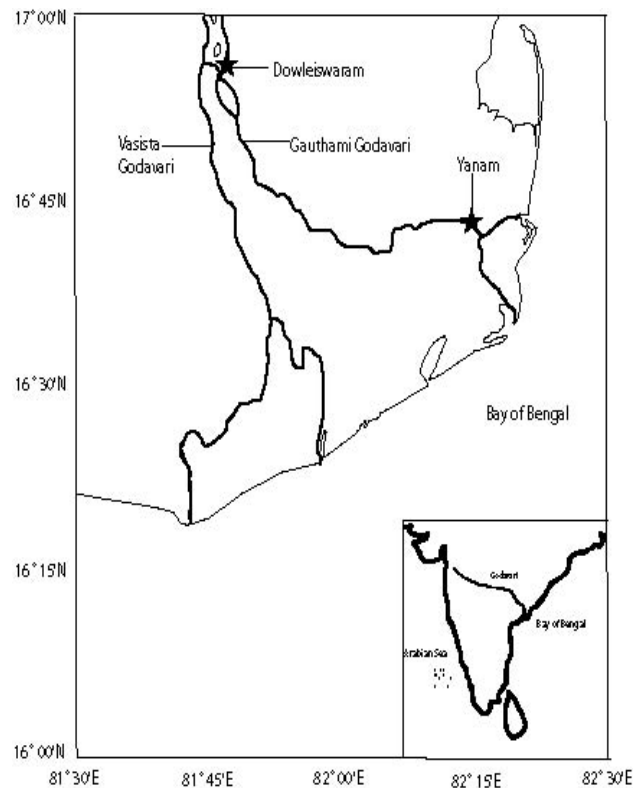


Figure 1: Station location.

## Material and Methods

The river Godavari originates in the Western Ghats near Nasik city at an altitude of about 1620 m and flows eastwards through Godavari garben and joins into Bay of Bengal (Fig. 1). This is the third largest estuary in India and receives significant amount of fresh water from the upstream river. At Dowleiswaram, it divides into two branches, Gautami and Vasishta and the Gautami branch

splits into two channels at Vrudha entrance but the majority of the flow is along the main channel which confluences at Bhairavapalem into Bay of Bengal. Gautami-Godavari estuary is a drowned river valley type of estuary<sup>22</sup>. Fresh water discharge is controlled by a century old “Low Dam” at Dowleiswaram and varies between 0 and  $>11000 \text{ m}^3 \text{ s}^{-1}$ <sup>23</sup>. Estuary is characterized by many Islands and creeks<sup>22</sup> with average width and depth of 1 km and 12 m, respectively<sup>24</sup>. Tides in the estuary are of semi-diurnal with the tidal range of 1 – 1.5 m. Estuary widens from upstream to mouth and many sills in the estuary are exposed during low tide.

Hourly time series data of CTD (SBE 19 plus seacat profiler, Make: Sea Bird Electronics, USA) which is having auxiliary sensors (Oxygen & Fluorescence) and currents at 10 min interval (3 m and 14 m) were collected approximately at the middle of the Godavari estuary (Yanam) (Fig. 1) for 2 days, 25-27 September 2008, using RCM 9 current meter (Anderaa Instruments, Norway). Daily river discharge data was obtained from dam authorities at Dowleiswaram (Fig. 1). Tides at an interval of 10 min were measured by a tide gauge, designed by Marine Instrument Division, NIO, Goa installed at Yanam. The methodology and computational procedure for deducing IW characteristics from the observed time series data has been explained in Appendix.

## Results and Discussion

The depth-time sections of temperature and salinity fields are shown in Figure 2. Since the focus of this paper is to document the IW characteristics either in the thermocline region or pycnocline region, the thermal and salinity structures in this figure, contoured at  $0.5^\circ\text{C}$  and 3 psu respectively. From these structures one can clearly see that no prominent and regular isotherm oscillations in the stratified water column (i.e. thermocline zone) (Fig. 2a). But, prominent and regular oscillations in salinity field in the stratified column are found within the inertial period (Fig. 2b). Such oscillations in salinity within the inertial period (42 hours) are caused by the local IW field<sup>25</sup>. Hence each isohaline in the pycnocline zone represents an IW. As such, the terms isohaline and IW are synonymously used in this paper. Figure 3 represents ensemble mean profiles of temperature ( $^\circ\text{C}$ ), salinity (psu), density ( $\text{Kg m}^{-3}$ ), Oxygen ( $\text{ml l}^{-1}$ ),

fluorescence ( $\text{mg m}^{-3}$ ) and  $N$  (cph) obtained from time series CTD data for understanding the physical process with the biological and chemical response. Surface temperature was found to be  $29.87^\circ\text{C}$  and mild temperature fall of  $0.25^\circ\text{C}$  observed upto depth of 2 m. Here, configuration of salinity profile is influenced by heavy fresh water discharge and tidal forcing.

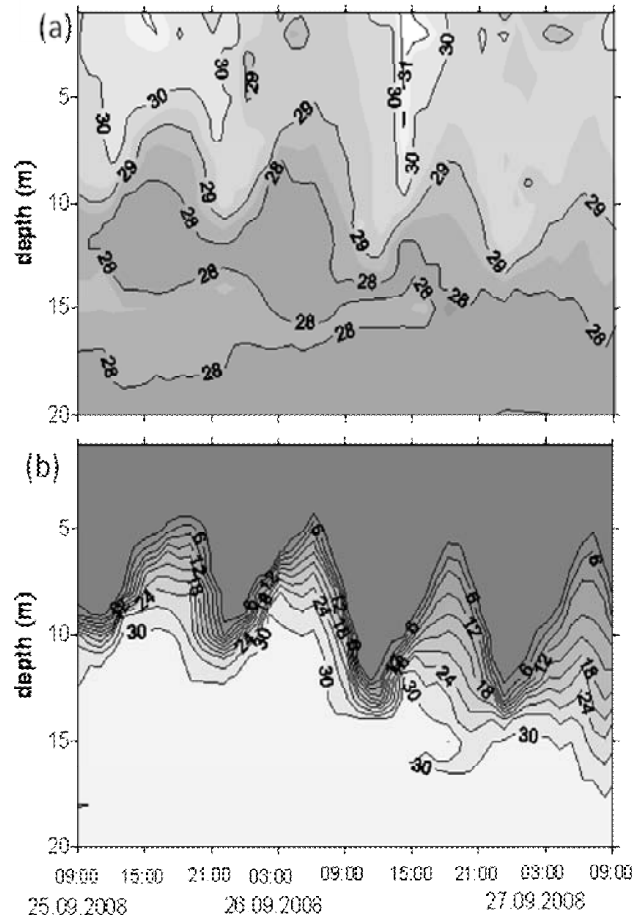


Figure 2: Vertical distribution of temperature (a) and salinity (b) in the Godavari estuary (at Yanam  $82.212^\circ\text{E}$   $16.716^\circ\text{N}$ ).

Isohaline (mostly fresh water) occurs up to a depth of 4 m due to fresh water discharge and below it is prevailing sharp gradient ( $25 \text{ psu m}^{-1}$ ) to the depth of 14 m. Overall the surface and bottom layer densities in the study area remain basically homogeneous during the observational period. The surface layer consists of fresh water with a density of  $\rho_1 = 995.94 \text{ kg m}^{-3}$  (salinity of 0.3 psu and temperature of  $29.83^\circ\text{C}$ ) whilst the bottom layer consists of salty water with a density of  $\rho_2 = 1019.19 \text{ kg m}^{-3}$  (salinity of 30.65 psu, temperature

of 27.86°C). These two layers are separated by a well-defined pycnocline that has an average thickness of 10 m. However, two exceptions are observed with respect to the bottom layer. It is well known that the strongly-stratified fluids (i.e.,  $\rho_1 \ll \rho_2$ ) have higher frequency oscillations, because the restoring force for vertical displacements is larger; for weakly stratified fluids, the opposite is true<sup>26</sup>.  $N$  is a measure of vertical stratification in the water column. Phillips<sup>27</sup> noticed that  $N$  represents a maximum value when the thermocline (or pycnocline) is at its greatest variation, and decreases above and below it. When  $N$  is a maximum, there are a finite number of modes<sup>25</sup>. It is the vertical frequency excited by a vertical displacement of a parcel of fluid. Depending on the strength of the stratification, the fluid parcel requires number of cycles to restore itself to equilibrium. In the present case, the  $N$  profile contains a peak at 96.67 cph in the pycnocline region due to high stratification. The number of peaks in the  $N$  profile also indicate the number of significant modes in the IW structure<sup>25</sup>. For example, profile is having two modes; one is at a depth of 10 m (96.67 cph) and second at depth of 14m (71.15 cph) although they cannot really define the mode composition of the IW.

In Figure 3, one can see that profiles of temperature, oxygen and fluorescence show similar trend. Profiles of salinity and density are increasing with depth and those are following law of proportionality, but inverse relationship with temperature, oxygen and fluorescence. Ensemble average of fluorescence and Oxygen were found to be higher (1.61 mg m<sup>-3</sup>, 5.28 ml l<sup>-1</sup>) in the surface layer contrast with bottom layer (0.52 mg m<sup>-3</sup>, 4.62 ml l<sup>-1</sup>). Surface to bottom difference in temperature and salinity are about 2°C and 31 psu respectively. This small difference in temperature and larger in salinity contributes about 24 kg m<sup>-3</sup> of density difference from surface to bottom. Fluorescence which represents chlorophyll is gradually decreasing from surface to bottom following the decrease of the availability of Oxygen. Here the surface to bottom oxygen difference is about 0.688 ml l<sup>-1</sup> and even > 4 ml l<sup>-1</sup> of oxygen is noticed in the water column which means that there is no hypoxic conditions were noticed for this water column which was noticed in other waters like Chesapeake Bay etc. Higher  $N$  values occur when there is a higher frequency in the oscillation of the fluid

parcel in the water column. This is associated with a higher vertical stratification or stability of the water column which was noticed at the depth of 10 m from surface. To know about the dynamics of water column and deducing and interpreting IW characteristics, figure 4 has been plotted.

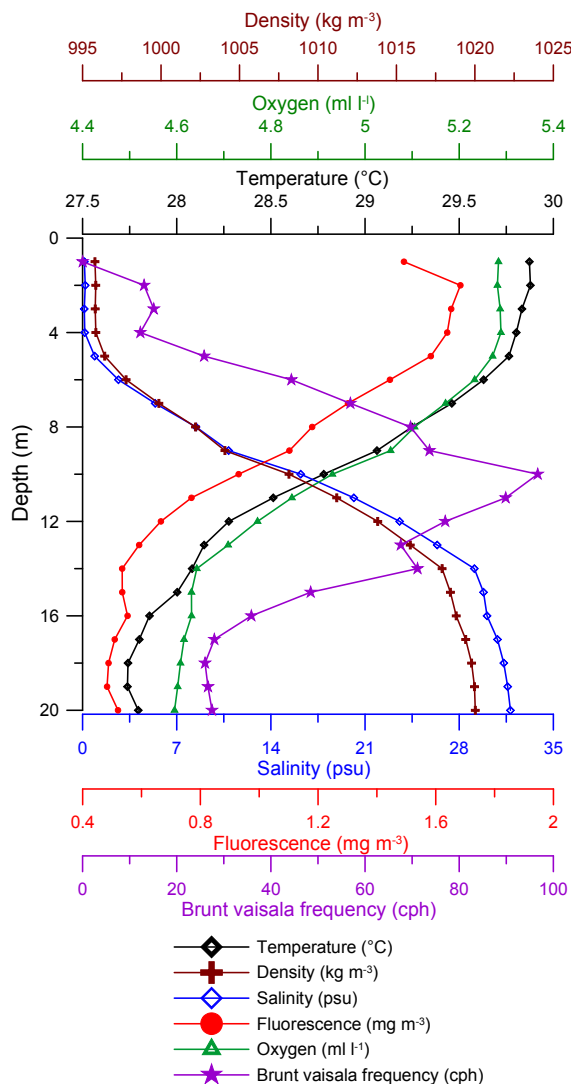


Figure 3: Temporal mean profile of temperature, salinity, density, Fluorescence, Oxygen, Brunt-Vaisala frequency off Godavari estuary (at Yanam).

### Currents

During the observational period, two layer structure exists in the estuary with surface water flowing towards seaward and landward flow at the bottom (Fig. 4a). Surface zonal velocity is nearly 10 times higher than the bottom zonal current but there is not much difference in the meridional current (Fig. 4b) which are much weaker. No systematic oscillations

are observed in meridional component (Fig. 4b). During low tide, the bottom zonal current is decreasing with increasing of surface current and this is opposite during high tides with some time lag to surface current (Fig. 4a). Overall the surface and bottom layer densities in study area remain basically homogeneous (where the current meter are deployed) for the duration of observed period. However, two exceptions are observed with respect to the bottom layer. First, the deeper depth area (where the depth reaches >14 m) has the densest bottom waters in the whole section. In this area, ensemble average surface current (-2.74 cm s<sup>-1</sup>) is inconsiderably small in contrast to the surface flow velocity (56.61 cm s<sup>-1</sup>) throughout the tidal cycle indicating that there is little or no mixing of these waters with water from upstream or downstream.

The surface zonal flow is unifying direction always towards sea ward with velocities varying between 20 cm s<sup>-1</sup> to 85 cm s<sup>-1</sup> (mostly driven by gravity driven force of fresh water (Fig. 4a)). Signatures of tidal force on zonal oscillations have been masked and those are unable to seen in figure 4a. But at the bottom, it has been noticed that oscillations in zonal currents which were varying between -20 cm s<sup>-1</sup> to 20 cm s<sup>-1</sup> are mainly following the tide rather than fresh water discharge. Surface turbidity is much higher than at the bottom turbidity which was further increases with increase of surface zonal velocity (Fig. 4c). The surface resembles with tidal force whereas bottom turbidity is independent of tidal force (Fig. 4c).

*Spectrum analysis*

Time series data have been subjected to Fast Fourier Transform (FFT) algorithm<sup>28</sup> to examine the spectral characteristics of the temperature oscillations<sup>29</sup>. Power spectra of u & v components of current oscillations at 3m and 14 m (Figs. 4a & 4b) are computed and presented in Figures 4d & e. Here the current meter data on speed, direction and turbidity have been recorded at 10 min interval. Results of spectrum with those data sets yield upto 3 cph frequencies and having energies more than 99 significance level which were considered for frequency analysis (Figs. 4d & 4e). This is useful to identify the distribution of the current of various frequencies. There is a broad range of wave-frequencies and associated energy, where waves of LF (<0.5 cph) are associated with high energy while those of HF (>0.5 cph) have low energy. The energy associated with the LF for both the depths is a measure of the effect of stratification, while it doesn't seem to have a definite bearing/relation on the HF counterpart. However, power spectra energy at bottom is relatively lower to that of surface. This phenomenon may be due to the high stratification of water column at surface (Figs. 3 & 4a).

*IW forming factors (sources)*

IWs are generated in regimes where the barotropic tidal current encounters irregularities in bottom topography. The topography acts as wave-maker owing to oscillatory “to and fro” motions associated with tidal cycles. The individual elements comprising this IW wave-forming scenario are (1) stratification, (2) tidal influences, (3) topographic influences and (4) perturbing and restoring forces etc. It has been demonstrated here that IWs can be generated by a river plume, and this

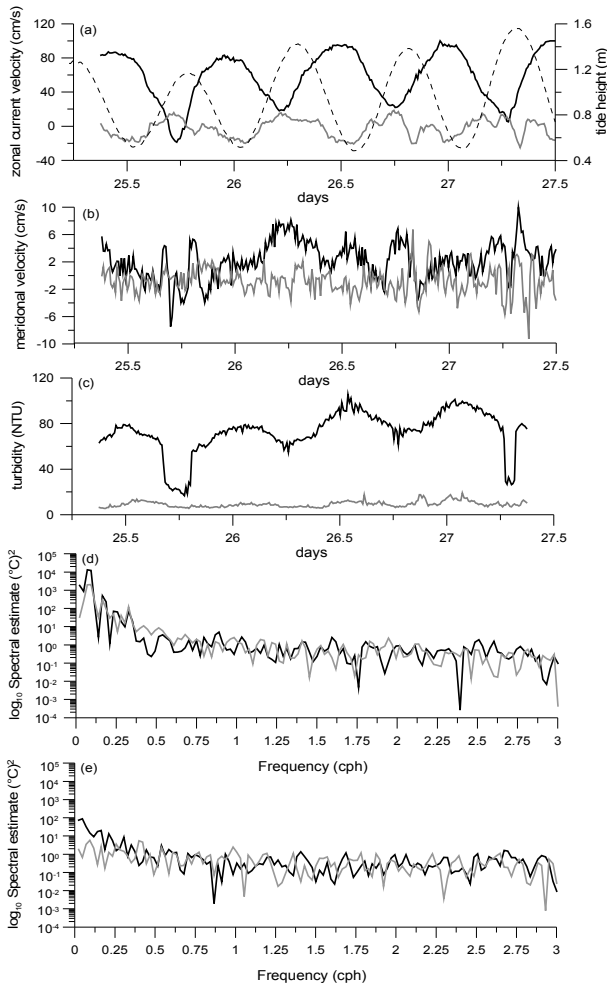


Figure 4: Time series data of (a) zonal velocity, (b) meridional velocity, (c) turbidity, (d) Spectral estimation of (c) zonal and (d) meridional velocities respectively. (Note: black line – surface (3 m); grey line – bottom (14 m); dashed line – tide).

mechanism works in a broad range of the background conditions when there driving forces, that is tidal flow, river discharge and horizontal density gradient act together, separately or in various combinations.

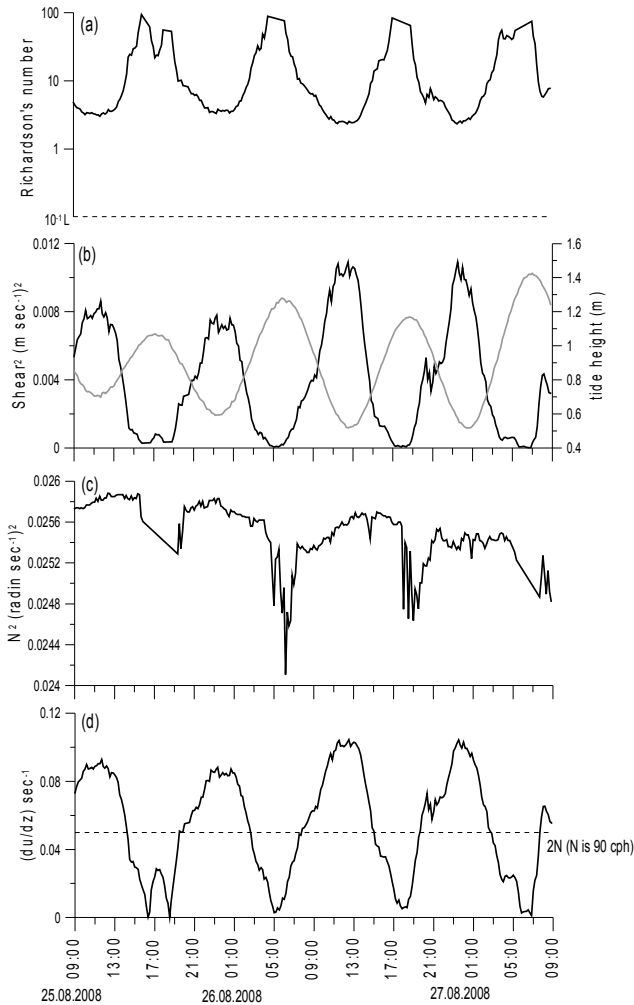


Figure 5: Variations of (a) Richardson number, (b) Square of shear, (c) square of Brunt-Vaisala frequency and (d) zonal velocity gradient & twice of Brunt-Vaisala Frequency.

*Stability of the water column*

In order to know the stability of the water column at the observation site and the probable mixing during the study period, Richardson Number ( $R_i$ ) (Fig. 5a), square of vertical shear (Fig. 5b),  $N^2$  (Fig. 5c), velocity gradient (Fig. 5d) were computed using the surface (3 m) and bottom (14 m) currents and CTD data from the following formulae:

$$R_i = \frac{N^2}{\left(\frac{\partial u}{\partial z}\right)^2} \dots\dots\dots (1)$$

Where

$$N = \sqrt{\frac{-g\partial\rho}{\rho_0\partial z}} \dots\dots\dots(2) \text{ Here } g \text{ is the}$$

acceleration due to gravity,  $\rho_0$  is the average density and  $z$  is the vertical co-ordinate (positive upwards), and the denominator of the above equation (1) is the vertical shear squared. Physically, the Richardson Number is the ratio of stabilizing buoyant forces to destabilizing shear forces, in the presence of a velocity gradient, that varies with depth. When considering shear flow in equation (1), when it exceeds twice the

$$\text{stratification } (N) \text{ i.e., } \left|\frac{\partial u}{\partial z}\right| > 2N \dots\dots\dots(3)$$

then IWs can break to produce turbulence and turbulent mixing via a progression in K-H instability progression<sup>30</sup>.

The  $N$  shows no variations with time and it is indicating that the stability of the water column which is constant (Fig. 5c) during observation period. Whenever vertical shear is higher, then tide happens to be minimum and vice versa (Figs. 5b & 5d). Hence from Figures 5b, 5c & 5d, one can conclude that the mixing of water column has not been controlled by static stability and it is mostly depends on the dynamic stability (Fig. 5a) and which is function of tidal force. Figure 5d reveals that, the zonal velocity gradient with reference to the  $2N$  value happens to be lower during flood and higher during ebb period. According to equation (3), IWs break during ebb and that produces turbulence field hence leads to have/cause mixing. In the present case, it happens to be mean value of  $N=90$  cph, which comes under the band of HF IW field domain. Hence one can come to a conclusion that from our observations, tidally modulated HF IWs which are prevailing under high stratification conditions and it can be identified as one of the mechanisms for the generation of HF IWs. Figure 5a displays the variation of  $R_i$  with time. Miles<sup>31</sup> and Howard<sup>32</sup> found that transition to turbulent flow can be achieved theoretically when  $R_i$  locally falls 0.25 anywhere within the water column. Conversely, stability within the system is assured

$R_i(z)$  – the likelihood of turbulent mixing is small and stratified shear flow dominates. Richardson<sup>33</sup> suggests that the critical value at which mixing can occur in stratified environments is  $0 < R_{ic} < 1$ . Later theoretical investigations have been placed the critical value in the range  $0 < R_{ic} < 0.25$ , for the fastest growing instability<sup>31, 34</sup>. In the present study,  $0 < R_{ic} < 1$  is used to cover all the mixing events. Recent experimental and observational data indicated that the turbulence can survive when global  $R_i \gg 1$ <sup>35</sup>. In the present case (Fig. 5a), computed global  $R_i (\gg 1)$  is always much greater than critical  $R_{ic}$  ( $=0.25$ ) and indicating that the turbulence (generated with tidally inducted HF IWs) is very much survive during the observational period and also that is the resultant of shear by gravity driven currents under heavy discharge and some extent to stratified shear flow domination. In order to know the requirement of shear to initiate interfacial mixing in the different layers of the present system, we have computed parameter of minimum velocity shear  $\sqrt{(R_i N^2)}$  with our observations and it has been found to be  $0.05 \text{ s}^{-1}$  and it is greater than actual requirement of about  $0.04 \text{ s}^{-1}$ <sup>36</sup>.

From the spectrum analysis (subject to limited data) the present system exhibited frequencies of IWs upto 3 cph for both the current meters situated one at the surface and another is at the bottom. But based on the CTD data, it has been deduced/computed parameter of  $N$  is 90 cph (ensemble average). This value is given some sort of a clue on the upper limit of IW field. Time series data on currents have not been covered to complete the span of IW band frequency field (i.e., inertia to  $N$ ). According to computed values of Richardson number and  $N$ , system exhibited HF IW band of 0.5 cph to 90 cph. Logically, one can understand that the earlier prevailed propagation of LF IWs in the present environment system might have been a stage of transition into HF IW field which are taking place under mixing conditions of water column by process of entrainment. It has been well confirmed by the computed value of positive buoyancy force ( $FB = -g(\rho_2 - \rho_1) = 0.0236 \text{ m s}^{-2}$ ). Whenever  $FB$  is positive value then it happens to be resulting buoyancy force in the upward<sup>37</sup>. Since buoyant force is upward, the system is vertically unstable suggesting the opposite scenario to most

common density configuration encountered in nature; – a more-dense fluid layer rests above a less-dense layer thus encouraging strong vertical mixing (or gravitational overturning). In general, the frequency of wave increases with strengthening of  $FB$ . Rivers issue into the coastal ocean as tidally-modulated pulses of fresh water that form positively-buoyant currents. The evolving properties of these gravity currents are determined by the initial momentum at the river's mouth, interactions with coastal currents (Ex., EICC etc.) and winds, and by the Earth's rotation, which tends to turn the current to the right in the northern hemisphere. These factors all affect the location, propagation speed and sharpness of the gravity current front<sup>20</sup>.

#### *IW parameters*

Computational details of IW characteristics utilizing harmonic method (via PCA method) and also their energy estimates are described in the Appendix. The computed ensemble averages of IW field (covering observation period) of  $t_{per}$ ,  $\rho$ ,  $\rho_1$ ,  $\rho_2$ ,  $C_{vel}$ ,  $FB$ ,  $KE$ ,  $\beta$  and  $c_0$  are found to be  $0.342 - 41.723 \text{ hrs}$ ,  $1010.3 \text{ kg m}^{-3}$ ,  $996.0 \text{ kg m}^{-3}$ ,  $1019.0 \text{ kg m}^{-3}$ ,  $0.5412 \text{ km hr}^{-1}$ ,  $0.0236 \text{ m s}^{-2}$ ,  $36.747 \text{ J m}^{-2}$ ,  $0.0177$ ,  $0.1064 \text{ m s}^{-1}$  respectively. These computed estimates are independent of frequencies. It is interesting to know that the  $KE$  is extremely high in this estuary compared to coastal waters of Bay of Bengal<sup>12</sup>. This may be due to the flow of high river discharge with velocity of  $0.15 \text{ m s}^{-1}$  driven by gravity towards mouth. To conformity of mechanism prevailed in present highly stratified system for generation of HF IWs (apart from above said criteria) is the mixing of water column which one encountered during transition stage to breaking of LF IWs. For this purpose, the Form Number ( $F$ )<sup>38</sup> has been computed. The  $F$  can be used to characterize the tidal regime in terms of the magnitudes of four of the primary tidal constituents. It is defined as  $(K_1 + O_1)/(M_2 + S_2)$  where  $K_1$  and  $O_1$  are the diurnal components and  $M_2$  and  $S_2$  are the principal semi diurnal contributors. It is well known that if the  $F$  value is between 0.25 and 3.0 it indicates that mixed tidal regime with the lower the number the greater the influence on the semi diurnal forcing which results in two distinct high and low waters per day. The present data revealed  $F$  around 0.92, indicative of a current regime that is mixed, but with strong semi diurnal component. So,

one can conclude that the LF IWs energy might have been utilized to generate HF IWs due to cause of wave - to - wave interaction.

**Mode 1:** The IW parameters have been computed with  $N=96.67$  cph (peak at depth of 10m in Figure 3) from the method described in Appendix. The frequency  $N$  is the solitary maximum around 10 m suggests that the IW fields are of predominantly first mode. At a depth of 10 m HF (96.67) IW was found to move with a phase speed ( $c_i$ ) of  $0.13 \text{ m s}^{-1}$  and wave length ( $L$ ) of  $0.0056 \text{ km}$  (wave number =  $178.64 \text{ cycles km}^{-1}$ ) having energies of  $0.0006 \text{ J m}^{-2}$  (potential) and  $0.0027 \text{ J m}^{-2}$  (baroclinic). The reconstructed displacement function ( $\eta(z,t)$ ) with these parameters has been computed and shown in Figure 6a to study the impact of first mode IW propagation in the present environment. Figure 6a shows, positive nature of displacement function ( $\eta(z,t)$ ) and that is indicating upward of isohalines in the pycnocline zone due to propagation of first mode IW and can be represented as elevation-type IWs. This is happened due to upward buoyant force. This behavior is similar to soliton.

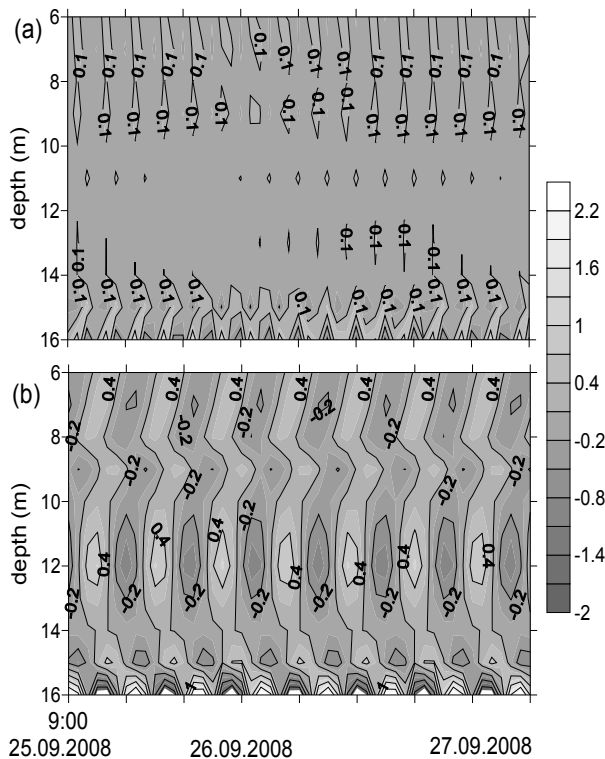


Figure 6: Distribution of internal wave displacement function for (a) mode 1 and (b) mode 2

**Mode 2:** The IW parameters have been computed with  $N=71.15$  cph (second peak at the depth of 14m in Figure 3) and these were found to be  $0.09 \text{ m s}^{-1}$ ,  $0.0076 \text{ km}$ ,  $131.48 \text{ cycles km}^{-1}$ ,  $0.0055 \text{ J m}^{-2}$ ,  $0.02 \text{ J m}^{-2}$  and  $0.094$  for  $L, \kappa, PE, BPE$  and  $C_i$  respectively. The reconstructed displacement function ( $\eta(z,t)$ ) with mode frequencies have been computed and shown in Figure 6b to study the impact of second mode IW propagation in the present environment. Figure 4 shows, oscillation nature of displacement of isohalines in the pycnocline zone due to propagation of second mode IW. Now one can conclude that the HF second mode IW is more energetic (8 times) (in contrast to first mode propagation) and is carrying chemicals (as described in the Figure 3) along with river plume towards estuary during the ebb time. Here one can notice that both waves have common factor that is moving with speed of sub critical wave speed range (i.e,  $C_i < C_0$ ).

Now one can conclude that the HF two modes of IWs are carrying chemicals along river plume pulses generated with these IWs entering towards estuary during the ebb time. One can anticipate that the river waters turns to the right/left just after leaving the mouth, which is in accordance with Coriolis effect. In the present case, the flow should be in the right to the shore. The flow of mass follows the local/general current system. For example, irrespective of the place where river plume leaves the estuarine mouth, flow of EICC impact on plumes can possible/ observed along the entire Indian coast aided by equator ward/poly ward during post and pre-monsoons respectively<sup>39</sup>. Recent studies,<sup>40, 41</sup> also showed the importance of EICC in the distribution of Chl-a along the east coast of India. These results of HF IWs characteristics (under three forces namely tidal flow, river discharge and horizontal density gradient) would be found more useful for validation/improvement of non-hydrostatic models of the present context.

## Conclusions

Present study describes the results from 2 days time series of CTD observations (sampled every hour) and currents data (sampled every 10 min interval) 3m and 14 m of the water column in the Godavari estuary (Yanam) during 25 - 27 September 2008. Observations were used to identify and retrieve/deduce IW characteristics and



their possible generation mechanism. Based on the analysis of spectrum, harmonic and stability criteria subject to limited time series data, results reveal that with identified two significant modes (1) first mode (96.68 cph at depth 10 m) : IW was found to move with a phase speed of  $0.13 \text{ m s}^{-1}$  and wave length of  $0.0056 \text{ km}$  (wave number= $178.64 \text{ cycles km}^{-1}$ ) having energies of  $0.0006 \text{ J m}^{-2}$  (potential) and  $0.0027 \text{ J m}^{-2}$  (baroclinic) where as (2) second mode (71.15 cph at depth 14 m)  $0.09 \text{ m s}^{-1}$ ,  $0.0076 \text{ km}$ ,  $131.48 \text{ cycles km}^{-1}$ ,  $0.0055 \text{ J m}^{-2}$ ,  $0.02 \text{ J m}^{-2}$  and  $0.094 \text{ m s}^{-1}$  for  $L$ ,  $\kappa$ ,  $PE$ ,  $BPE$  and  $c_i$  respectively. The  $\eta(z,t)$  was found to be positive (elevation-type IWs) and negative values (oscillation-type) during IW propagation of two modes respectively wherein mode two is more energetic (8 times) in contrast to mode 1: Tidally-modulated force is the possible mechanism to generate HF IWs during ebb period.

### Acknowledgements

Authors are grateful to Dr.S.W.A. Naqvi, Director and Dr.S.R. Shetye, former Director, NIO, Goa, Council of Scientific and industrial research (CSIR), New Delhi, India, for their interest in this study and for providing facilities. One of the authors (B.Sridevi) is grateful to CSIR for the grant of Junior Research Fellowship during the tenure of which a part of this work was carried out. This is NIO contribution number 5417.

### References

1. Wunsch C., & Ferrari R., Vertical mixing, energy, and the general circulation of the oceans. *Ann. Rev. Fluid Mech.*, 36, (2004) 281–314.
2. Rao, A.D., Babu, S.V., Prasad, K.V.S.R., Ramana Murty, T.V., Sadhuram, Y., Mahapatra, D.K., Investigation of the generation and propagation of low frequency internal waves: A case study for the east coast of India. *Estuar. Coast. Shelf. Sci.*, 88, (2010)143-152.
3. Lvov, Y., & Tabak, E., Hamiltonian formalism and the Garrett-Munk spectrum of internal waves in the ocean. *Phy. Rev. Lett.*, 87, (2001)168501.
4. Garrett, C., and Munk, W., Internal Waves in the Ocean. *Ann. Rev. Fluid Mech.*, 11, (1979) 339-369.
5. Munk, W., *Internal waves and small-scale processes. In evolution of Physical Oceanography*. Scientific surveys in Honor of Henry Stommel, ed. B.A. Warren and C.Wunch (1981) 265-291, Cambridge (MA), MIT press, USA.
6. Murthy, P.G.K., *An Insight into Internal Waves in the Seas – around India. International Conference on Sonar – Sensors and Systems*. In Proceedings of ICONS, Kochi, Naval Physical and Oceanographic Laboratory, India, (2002) 525-532.
7. La Fond, K.G., Rao, C.P., Vertical oscillations of tidal periods in the temperature structure of the sea. *And. Uni. Memor.*, 1, (1954) 109-116.
8. La Fond, E.C., La Fond, K.G., Studies on oceanic circulation in the Bay of Bengal. *But. of Nat. Ins. of Sci. India.*, 38, (1968) 169 -183.
9. Murthy, P.G.K., and James, V.V., *Some aspects of internal waves in the coastal waters off Cochin*. Proceedings of the Second workshop on the Scientific Results of FORV Sagar Sampada, (1996) 47-55.
10. Murthy, P.G.K., and Mohan Kumar, N., *Confirmatory checks for the internal waves in the coastal waters off Cochin*. Proceedings of the Second workshop on the Scientific Results of FORV Sagar Sampada, (1996) 39-45.
11. Krishna Kumar, G.V., and Murthy, P.G.K. *Internal wave characteristics in the coastal waters off Cochin in October 97*, Proceedings of the National Conference on Current trends in the ocean prediction with special Reference to Indian seas (Dec. 22-23, Kochi, India), (1998) 90-94.
12. Sridevi B., Ramana Murty T.V., Sadhuram Y., Rao M.M.M., Maneesha K., Sujith kumar S. and Prasanna P.L., Impact of internal waves on sound propagation off Bhimilipatnam, east coast of India. *Estuar. Coast. Shelf. Sci.*, 88, (2010) 249-259.
13. Sridevi, B., Murty, T. V. R., Sadhuram, Y., and Murty, V. S. N., Impact of internal waves on the acoustic field at a coastal station off Paradeep, east coast of India, *Nat. Haz.*, 57, (2011) 563- 576.
14. Rao A.D., Prasad K.V.S.R., and Ramana Murty, T.V., *Identification and Modelling of Internal waves-Phase II*. Joint Research Project, funded by Naval Research Board, DRDO, India, (2010).
15. Nash, J.D., and J.N. Moum., River plumes as a source of large-amplitude internal waves in the coastal ocean. *Nature.*, 437, (2005) 400–403, doi:10.1038/nature 03936
16. Wang, D.P., Tidally generated internal waves in partially mixed estuaries. *Cont. Shelf. Res.*, 26, (2006) 1469 -1480.
17. New, A.L. and Dyer, K.R., *Internal waves and mixing in the stratified estuarine flows.*, in : *Physical processes in estuaries*. 239-254, Dronkers et.al. (eds.), Springer-Verlag, Berlin (1988).
18. Philip, H., Kerstin, S. And Alexander, B., Generation and evolution of high-frequency internal waves in the Ems estuary, Germany. *J. Sea Res.*, 78, (2013) 25-35.
19. Richards, C., Bourgault, D., Galbraith, D.S., Hay, A., Kelley, D.E., Measurement of shoaling internal waves and turbulence in an estuary. *J. Geophys. Res.*, 118, (2013) 273-286.

20. Buckley, J.R., *A linear model for internal tides in sill Fjords, in Fjord Oceanography*. NATO conference series 4, (1980) 165-171, 10.1007/978-1-4613-3105-6\_6.
21. Stashchuk, N., and Vlasenko, V., Generation of internal waves by a supercritical stratified plume. *J. Geophys. Res.*, 114 (2009) (C01004).
22. Narasimha Rao TV, Time dependent stratification in the Gauthami-Godavari estuary. *Estuar. Coasts.*, 24, (2001) 18-29.
23. Sarma, V.V.S.S., S.N.M.Gupta, P.V.R.Babu, T.Acharya, N.Harikrishnachari, K.Vishnuvardhan, N.S. Rao, N.P.C.Reddy, V.V.Sarma, Y.Sadhuram, T.V.R.Murty, M.D.Kumar, Influence of river discharge on plankton metabolic rates in the tropical monsoon driven Godavari estuary, India. *Estuar. Coast. Shelf. Sci.*, Estuarine, coastal and shelf science 85, (2009) 515-524.
24. Reddy, BSR, and Ranga Rao V., Seasonal variation in temperature and salinity in the Gautami-Godavari estuary. *Proc. of Indian Acad. of Sci. (Ear. Plan. Sci.)*, 103, (1994) 47-55.
25. Roberts, J., *Internal gravity waves in the ocean*. New York, Dekker (1975).
26. Peter Lee Michael., *Numerical simulation of nonlinear internal solitary wave interactions with submarine topographic features*. Dissertation, Catholic university of America, Washington, D.C (2011).
27. Philips, O.M., *Internal waves (chapter 5) in "The Dynamics of the upper Ocean"*, Cambridge: Cambridge University Press (1966).
28. Cooley, J.W., Tukey, J.W., An algorithm for the machine calculation of complex fourier series. *Math. of Comp.*, 19, (1965) 297.
29. Mahadevan, R., Swaminathan, T., Issac Martin, M., *Ocean surface wave analysis*. Technical Report 27, Ocean Engineering center Indian Institute of Technology, Chennai, (1987) 115.
30. Criminale, W.O. Jr. *On breaking of internal gravity waves*. In Sciences of the U.S.S.R. International Symposium on stratified Flows held in Novosibirsk, August 29-31, 1972, 175-192. New York: American Society of Civil Engineers (1973).
31. Miles, J., On the stability of heterogeneous shear flow. *J. Fluid. Mech.*, 10, (1961) 96-508.
32. Howard, L.N. Note on a paper of John W.Miles. *J. Fluid. Mech.*, 10, (1961) 509-512.
33. Richardson, L.F., *The supply of energy from and to atmospheric eddies*. Proceedings of the Royal Society, London, A97, (1920) 354-373.
34. Miles, J. W., and L. N. Howard, Note on a heterogeneous shear flow. *J. Fluid. Mech.*, 20, (1964) 31-336.
35. Galperin, B., Sukoriansky, S., and Anderson, P.S., On the critical Richardson number in stability stratified turbulence. *Atm. Sci. Lett.*, 8, (2007) 65-69.
36. Delpeche, Nicole C., Tarmo Soomere and Madis-Jaak Lilover, Diapycnal mixing and internal waves in the Saint John river estuary, new Brunswick, Canada with a discussion relative to the Baltic sea. *Estonian J. Engg.*, (2010) 157-175.
37. Wojcik E.Stefanie, *Effects of Internal waves and Turbulent Fluctuations on underwater Acoustic Propagation*. Master of Science thesis, Worcester Polytechnic Institute (2006).
38. Dietrich, G., *General Oceanography: An Introduction*. Wiley-Inter- science, New York (1963).
39. Shetye, S.R., Gouveia, A.D., Shankar, D., Sheno, S.S.C., Vinayachandran, P.N., Sundar, D., Michael, G.S., Nampoothiri, G., Hydrography and circulation in the Bay of Bengal during the northeast monsoon. *J. Geophys. Res.*, 101, (1996) 14011-14025.
40. Vinaychandran P.N., Impact of physical processes on chlorophyll distribution in the Bay of Bengal; In: Indian Ocean Biogeochemical Processes and Ecological Variability. *Geophys. Mono. Ser.*, 185, (2009) doi:10.1029/2008GM000705.
41. Maneesha, K., Sarma, V.V.S.S., Reddy, N.P.C., Sadhuram, Y., Murty, T.V.R., Sarma, V.V., DileepKumar, M., Meso-scale atmospheric events promote phytoplankton blooms in the coastal Bay of Bengal. *J. Ear. Sys. Sci.*, 120, (2011) 773-782.
42. Murthy, P.G.K. and Murthy, G.R.K., A case study on the influence of internal waves on sound propagation in the sea. *J. Sound. Vib.*, 108, (1986) 447.
43. Defant, A., *Physical Oceanography*. volume 2. Oxford Pergamon Press, (1961) 517- 526.
44. Stephen, M.Chiswell., Tidal Energetics over the Chatham Rise. New Zealand. *J. Phys. Oceanogr.*, (2000) 2452-2460.
45. Liebelt, P.B., *An Introduction to Optimal Estimation*. Addison-Wesley Publishing Company, London, (1967) 272.
46. Menk W., *Geophysical data analysis: Discrete Inverse Theory*. 2<sup>nd</sup> ed Academic Press, San Diego (1989).
47. Aki, K., and Richards, P.G. *Quantitative Seismology, theory and methods*. W.H. Freeman, San Francisco (1980).
48. Park J.H., *Study on the analyses of the Coastal Acoustic Tomography Data*. Doctor Dissertation, Graduate School of Engineering, Hiroshima University, (2001).
49. Ramana murty, T.V., Veerayya, M., and Murty C.S., Sediment size distribution of the beach and near shore environs along central west coast of India: An analysis using EOF. *J. Geophys. Res.*, 91, (1986) 8523-8526.
50. Ralston, A. and Wilf, H.S., *Mathematical methods for digital computers, Spline functions, Interpolation and numerical quadrature*. T.N.E. Greville, (1967)156-168.

**Appendix**

**Methodology and Computational procedure**

Typical vertical scales of IW are around 10 m and the horizontal scales vary from few hundreds meters to kilometers. Temporal scales are of the order of hours, bounded by a minimum frequency at the inertial frequency ( $f$ ) (a function of latitude) and a maximum frequency at the  $N$ . With in the above frequencies, IW characteristics like amplitudes, velocities, wave length, wave number, energies were computed following the earlier studies<sup>42, 43, 44</sup>. The waters in the pycnocline are stratified i.e., least turbulent. When these waters are disturbed by an external force (winds, surface waves, tides, etc) and internal force (shear associated with currents, bottom force etc) they respond through manifestation of IW.

To compute IW wave number ( $k = 2\pi/L$ ),  $L = C_{vel}t_{per}$ , where  $L$ ,  $C_{vel}$ ,  $t_{per}$  are wave length, velocity and period respectively),  $L$  is needed. To compute  $L$ ,  $C_{vel}$  and  $t_{per}$  are needed.  $C_{vel}$  is computed using two layer density model<sup>43</sup> as  $C_{vel}^2 = gh_1(\rho_2 - \rho_1) / \rho_2$  where  $h_1$  is the thickness of the top layer of weak density gradient,  $\rho_2$  is density of bottom layer of strong density gradient,  $\rho_1$  is the mean density of top layer of weak density gradient and  $g$  is the acceleration due to gravity. This depth-density relationship is allied for system in the shallow fluid. Another parameter of IW is phase speed ( $c_i = c_0 + 4\beta/\lambda^2$ ). To compute IW phase speed ( $c_i$ ), both coefficient of dispersion ( $\beta$ ) and wave celerity ( $c_0$ ) are needed. When taking into account the densities of the respective fluid layers and those parameters are defined as:

$$c_0 = \left[ \frac{g(\rho_2 - \rho_1)h_1h_2}{\rho_2h_1 + \rho_1h_2} \right]^{\frac{1}{2}} \quad \beta = \frac{c_0}{6} h_1h_2$$

The ideal IW speed or celerity  $C$  can be calculated for any particle located along the interfacial density surface (defined by above relationship) assuming a small infinitesimal difference in density. A (actual) phase velocity  $c$  that results from the numerical simulation can also be calculated by selecting a fixed particle location along the density interface (pycnocline) and measuring the time differential  $\Delta = t_2 - t_1$  it takes

for that particle to travel some defined distance . In this manner, the phase velocity can be expressed as  $c = \Delta x / \Delta t$ <sup>26</sup>.

An insight into IWs in the seas around India was reviewed by Murthy<sup>6</sup> and found that the IW frequencies extending from inertial frequency to semidiurnal frequency – internal tides - dominate the LF band of IW, while IW of > 0.5 cph (0.005 hrs) dominate the HF band of IW. In the present study, the simulation is carried out to study the impact of HF IW field on system covering from ( $\omega_i = 0.5cph$ ) to buoyancy frequency ( $N = 90cph$ ). IW Energy ( $E_0$ ) can be estimated from the in-situ time series data. In order to compute  $E_0$ , amplitudes and phases of IWs are needed. This is done by adoption of Harmonic analysis.

**Harmonic analysis:** This approach determines to what extent the variations in the time series match the oscillations of the constituents that are known to exist in the tidal regime. The procedure adjusts the magnitude and timing (phase) until the best fit (assessed using a least square criterion) is achieved. The output of the analysis provides a list of frequencies that correspond to the frequencies of the tidal components, with an associated magnitude and phase. The greater the magnitude the greater the influence that a particular tidal constituent has on the time series.

For this purpose, the temperature ( $T(z,t)$ ) and vertical displacement ( $\eta(z,t)$ ) of pycnocline due to IW, expressed in terms of ensemble mean  $\bar{T}(z)$ , tidal constituents ( $\omega_i$ ) are estimated following Stephen<sup>44</sup> (in the present case, since isohaline in the pycnocline zone represents an IW field, we have taken salinity time series data instead of temperature):

$$T(z,t) = \bar{T}(z) + \sum_{i=1}^n T_i(z) \cos(\omega_i t - \phi_i^T(z)) \dots (1) \text{E}$$

Equation (1) has parameters  $a_i$ ,  $b_i$  and  $\omega_i$ . We will assume that  $\omega_i$  is known. Expanding Eq.1 we get

$$T(z,t) - \bar{T}(z) = \sum_{i=1}^n (a_i \cos \omega_i t + b_i \sin \omega_i t) \dots (2)$$

$$a_i = T_i(z) \cos \phi_i^T, b_i = T_i(z) \sin \phi_i^T \text{ and } \eta_i(z) = T_i(z) / (\partial \bar{T} / \partial z)$$

Using criteria of minimizing the sum of squares of the errors we minimize

$$S = \left( \sum (T(z,t) - \bar{T}(z)) - \sum_{i=1}^n (a_i \cos \omega_i t + b_i \sin \omega_i t) \right)^2 \dots\dots\dots (3)$$

Taking the partial derivatives of s with respect to  $a_i$  and  $b_i$  and setting them equal to zero we obtain the following normal system of normal equations:

$$Ax = D \dots\dots\dots (4)$$

$$A = B^T B \dots\dots\dots (5)$$

$$B = \left( \sum_j^k \cos \omega_j t_j, \sum_j^k \sin \omega_j t_j, \dots, \sum_j^k \cos \omega_j t_j, \sum_j^k \sin \omega_j t_j, \dots, \sum_j^k \cos \omega_j t_j, \sum_j^k \sin \omega_j t_j \right) \dots\dots\dots (6)$$

$$x = (a_1, b_1, \dots, a_n, b_n)^T \dots\dots\dots (7)$$

$$D = \sum_j^k (T(z, t_j) - \bar{T}(z)) \dots\dots\dots (8)$$

where  $z$  is the depth array,  $t$  is the time array of  $k$  elements,  $n$  is the number of tidal frequency. In Eq.6, matrix  $B$  is row vector consisting of  $2n$  elements having consequent trigonometric cosine and sine functions. Eq. (4) is solved for  $x$ - array which consisting of model parameters by appropriate inverse techniques. The least square method, damped least square method and Gauss-Markov method are introduced as suitable inversion techniques for geophysical applications. The Gauss-Markov method<sup>45</sup> has been used as the familiar technique. However, in the case of lack of statistical information, the least squares method may be an alternative to be selected. When the least squares method has problems related to smaller eigen values for coefficient matrix (data kernel), it is to be replaced by PCA<sup>46-48</sup>. In this study simulation PCA has been applied.

**Principal Component Analysis (PCA):**

Data kernel  $A$  of order  $(2n \times 2n)$  defined in equation 5 is expressed as a product of three matrices  $A = U \Gamma U^T \dots\dots\dots (9)$

The columns of the  $U = \{u\}$  matrix are orthonormal, i.e.,  $U U^T = I_{2n}$ . In general,  $U U^T \neq I_{2n}$ .  $U$  is the eigen vector matrix of  $A$  for the eigen value problem defined as

$$(A A^T) u = l^2 u \dots\dots\dots (10)$$

In Eq. (9),  $\Gamma$  is a diagonal matrix of non-zero singular values ( $l^2$ ) of  $A$  arranged in decreasing order, and  $r (\leq 2n)$  is the rank of the matrix. Once  $U$  and  $\Gamma$  obtained by solving above eigen value problem (Eq. 10), the generalized inverse solution follows as  $x = U \Gamma^{-1} U^T D \dots\dots\dots (11)$

For better estimates, it is done by judiciously selecting the  $p$  eigenvectors or ranking the singular values of the data kernel ( $A$ ) in a descending order. The noise in the data kernel prevailing in the form of small eigen values increases the ranking of the matrix apart from amplifying the solution. This, however, does not provide any additional or useful information on the model parameters. So, it can be treated as taught the solution to the present problem is obtained through consideration of optimization.

**Closeness Ratio:** The ratio of the sum of the factor model to that of the data matrix is considered as a measure of closeness of the model data<sup>49</sup>. Measure

$$\text{of closeness} = \frac{\sum_{i=1}^p l_i^2}{\sum_{i=1}^r l_i^2} \dots\dots\dots (12)$$

Where  $p$  is the number of factors considered and  $r$  is the rank of the data matrix. The first eigen function associated with the largest eigen value represents the broader features in the data, in the least square sense; while the second function and so on describe the residual mean square data. The closeness ratio expressed in percentage enables one to judge the contribution of different modes, and thereby reproduce the model profile.

Once PCA solution  $x$  is obtained, one can obtain amplitudes ( $\tau_i$ ) and phases ( $\phi_i$ ) as

$$\text{follows } \tau_i = \sqrt{(a_i^2 + b_i^2)} \dots\dots\dots (13)$$

$$\Phi_i = \tan^{-1}(a_i / b_i) \dots\dots\dots (14)$$

The vertical displacements  $\eta(z, t)$  for each tidal constituent can be estimated in the following Eqn. (15) by dividing the amplitude functions by the vertical gradient i.e.,  $\eta_i(z) = \tau_i / (\frac{\partial \bar{T}}{\partial z})$ .

$$\eta(z, t) = \sum_{i=1}^n \eta_i(z) \cos(\omega_i t - \phi_i^\eta(z)) \dots\dots\dots (15)$$

The functions of  $\phi_i^T(z)$  and  $\phi_i^\eta(z) (= \phi_i^T + \pi)$  represent phases corresponding to temperature/salinity and displacement. For example, in a two-layered system defined by  $h_1$  and  $h_2$  (respective fluid layers have densities  $\rho_1$  and  $\rho_2$ ), the displacement parameter  $\eta(t)$  represents the IW profile and is the interfacial surface which two fluid layers meet. IWs can be mechanically-generated (or naturally) and evolve into IWs as a result of advection and dispersive forces. IWs elevation/depression are typically associated with depth scenarios defined by  $h_1 > h_2$  ( $h_1 < h_2$ )<sup>26</sup>. Once amplitudes and phases of

displacement function ( $\eta(z, t)$ ) of IWs are computed,  $E_0$  [= Potential Energy ( $PE$ ) + Kinetic Energy ( $KE$ ) + Baroclinic potential energy ( $BPE$ )] can be estimated<sup>37</sup> as follows:

$$\langle PE \rangle = \frac{1}{2T_0} \int_0^T \rho g \eta^2(t) dt \text{ and } \dots\dots\dots(6)$$

$$\langle KE \rangle = \frac{1}{2T_0} \int_0^T \rho H (u^2(t) + v^2(t)) dt \dots\dots\dots(7)$$

$$\langle BPE \rangle = \frac{1}{T} \int_0^T \frac{1}{2} \int_{-H}^0 \rho(z) N^2(z) \eta^2(z, t) dz dt \dots\dots\dots(18) \text{ where}$$

$\eta, u, v, T, \rho, H, N$  are the displacement profile, zonal and meridional currents, observational period, density, water depth and Brunt-Vaisala frequency respectively. Here  $\langle \rangle$  indicates ensemble average. Eqn. (16-18) have been performed by cubic spline method<sup>50</sup>.